Viscoelastic Relaxation of Styrene−Butadiene Diblock Copolymer Micellar Systems. 2. Behavior in Entangling, Long Polybutadiene Matrices

Hiroshi Watanabe,* Tomohiro Sato, and Kunihiro Osaki

Institute for Chemical Research, Kyoto University, Uji, Kyoto 611, Japan

Received August 24, 1995[⊗]

ABSTRACT: For blends of styrene−butadiene (SB) diblock copolymers in entangling, high-M homopolybutadiene (hB) matrices, two-step viscoelastic relaxation behavior found in a previous study (Watanabe, H.; Kotaka. T. *Macromolecules* **1984**, *17*, 342) was reexamined to elucidate features of the fast process on the basis of recently accumulated knowledge for relaxation of homopolymer blends. The SB/hB blends contained spherical micelles with S cores and B corona. For the fast process, the micelles exhibited nearly universal dependence of reduced moduli, $G_r^* = [M_{bB}/c_{bB}RT]G^*_{SB}$, on reduced frequencies, $\omega\tau^*$, with c_{bB} and M_{bB} being the concentration of the B blocks in the hB matrix and the B block molecular weight, respectively, and τ^* being the relaxation time of the fast process. Behavior of τ^* changed with M_{bB}, c_{bB}, and the matrix molecular weight M_{hB}. For *dilute* micelles with $c_{bB} < c_e$ (entanglement threshold for the B blocks), the B blocks were entangled only with the hB matrix and τ^* were found to be close to constraint release (CR) relaxation times τ_{CR} evaluated from data for star-hB blends. This result led us to attribute the fast process of the dilute micelles to CR relaxation of the B blocks due to the matrix motion. On the other hand, for concentrated micelles with $c_{bB} > c_e$, the B blocks were entangled with both hB matrix chains and B blocks of neighboring micelles. For $M_{bB} \gg M_{hB}$, τ^*_{conc} of the concentrated micelles were longer than τ_{CR} and increased exponentially with c_{bB}. For those micelles, τ^*_{conc} agreed well with those in a nonentangling matrix. However, with increasing $M_{hB} \rightarrow M_{bB}$, τ^*_{conc} became insensitive to c_{bB} and approached τ_{CR}. These results for the concentrated micelles were similar to those for homopolymer blends, suggesting that the CR mechanism affected the fast process of those micelles in the following way: For $M_{bB} \gg M_{hB}$, the CR relaxation was rapid and entanglement between the matrix and the B blocks did not survive at time scales of τ^*_{conc}. Thus, at those time scales, the hB matrix behaved just as a diluent and the B blocks relaxed with a starlike (arm retraction) mechanism similar to that in the nonentangling matrix. On the other hand, for large M_{hB}, the CR relaxation was retarded and the entanglement with the matrix still survived at time scales of τ^*_{conc}. For this case, the CR relaxation became a rate-determining step for the B block relaxation and led to the c_{bB}-insensitive τ^* ($\cong \tau_{CR}$).

I. Introduction

In part 1 of this series of papers,[1] we have reexamined previous viscoelastic data of Watanabe and Kotaka[2] for blends of styrene−butadiene (SB) diblock copolymers in a short homopolybutadiene (hB) matrix. The blends contained spherical micelles with S cores and B corona. Those blends exhibited fast and slow relaxation processes. Comparing features of the fast process with those for relaxation of star chains, we attributed this process to starlike, arm retraction of entangled B blocks that was retarded by the S cores behaving as an impenetrable wall for the B blocks.[1]

In the blends examined in part 1, the short chB-2 matrix (M = 2K) provided no entanglement effect for the B block relaxation. This effect is naturally expected for the SB micelles in long hB matrices. More than ten years ago, Watanabe and Kotaka[3] also studied viscoelastic behavior of SB blends in such long, entangling hB matrices. These blends exhibited fast and slow relaxation processes, as similar to the blends in the short, nonentangling matrix. Watanabe and Kotaka[3] focused their attention to the terminal relaxation (slow process) and did not specify features of the fast process in the entangling matrices. On the basis of data for entanglement relaxation of homopolymer blends[4−17] accumulated mostly in the past ten years, we can now specify those features and examine mechanisms for the fast process of the SB blends in the entangling hB matrices. From this point of view, we have reanalyzed the previous data[3] for the SB blends. This paper presents the results, placing emphasis on features of the fast process.

Table 1. Characteristics of SB and hB Samples

code[a]	$10^{-3}M_S$	$10^{-3}M_B$	M_w/M_n
	SB Diblock Copolymer[b]		
SB 32−102 (SB3)	32	102	1.07
SB 32−160 (SB4)	32	160	1.08
SB 32−262 (SB5)	32	262	1.10
	hB Matrix[b]		
hB−28 (hB1)		27.6	1.05
hB−61 (hB2)		60.7	1.05
hB−177 (hB3)		177	1.06

[a] Parentheses indicate the previously used sample code.[3] [b] 1,2-Vinyl:1,4-cis:1,4-trans ≅ 10:40:50 for the B blocks and hB matrices.

II. Experimental Section

Table 1 summarizes the molecular characteristics of the styrene−butadiene (SB) diblock copolymers and homopolybutadiene (hB) matrices used in a previous study.[3] They were anionically synthesized in benzene, and the B blocks and hB matrices had the typical microstructure, 1,2-vinyl: 1,4-cis:1,4-trans ≅ 10:40:50. The hB matrices had M_{hB} well above the characteristic molecular weight for entanglement, M_c^0 = 6K. These matrices were entangled with the B blocks irrespective of the SB content.

For SB/hB blends containing spherical micelles with S cores and B corona, viscoelastic data were obtained in the previous

[⊗] Abstract published in *Advance ACS Abstracts,* December 1, 1995.

0024-9297/96/2229-0113$12.00/0

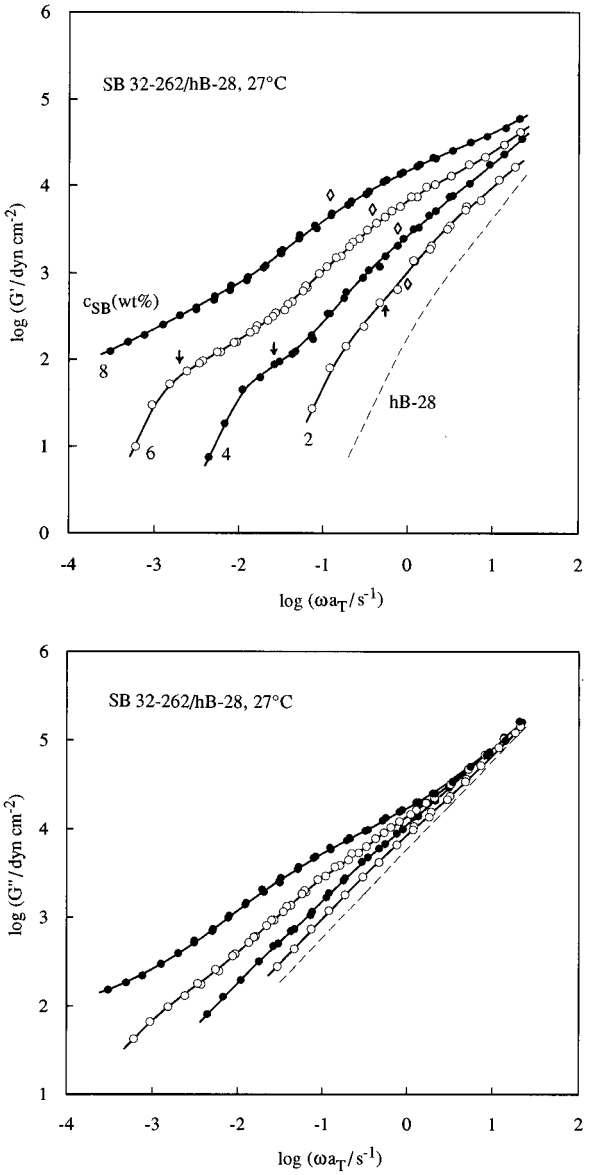

Figure 1. Frequency dependence of G' and G'' for SB 32−262/hB-28 blends[3] at 27 °C. Diamonds and arrows indicate characteristic frequencies, τ^{*-1} and τ_s^{-1}, for the fast and slow processes, respectively.

study.[3] Differing from the chB-2 matrix examined in part 1, the high-M_{hB} hB matrices used here were 1,4-rich hB chains. Thus, the data for the SB/hB blends at 27 °C[3] can be directly compared with data (at 27 °C) obtained by Roovers[17] for blends of 1,4-hB star chains in 1,4-hB linear matrices. The data for the SB/hB blends were compared also with the data for the SB/chB-2 blends[1] that were reduced at an isofrictional state.

III. Results and Discussion

III.1. Overview. Figure 1 shows representative G' and G'' data at 27 °C obtained in a previous study[3] for SB 32−262/hB-28 blends containing randomly dispersed spherical micelles with S cores and B corona. The corona B blocks are entangled with the matrix hB chains irrespective of the SB content c_{SB}. For $c_{SB} \geq 4$ wt %, the B block concentration c_{bB} in the hB matrix phase is well above the entanglement threshold $c_e = \varrho_{bulk} M_e^0 / M_{bB}$, with ϱ_{bulk} and M_e^0 being the density and entanglement spacing for bulk hB and M_{bB} being the B block molecular weight. Thus, for $c_{SB} \geq 4$ wt %, neighboring micelles are entangled through their corona B blocks.

As seen in Figure 1, the SB 32−262/hB-28 blends exhibit fast and slow relaxation processes. Both processes are retarded as the neighboring micelles are more heavily entangled (with increasing $c_{SB} \geq 4$ wt %). Similar results were found in part 1 also for blends in the nonentangling matrix.[1]

As done for homopolymer blends,[7−12] contribution of the SB micelles to G^*_{blend} of the blends is evaluated as

$$G^*_{SB}(\omega) = G^*_{blend}(\omega) - \phi_{hB} G^*_{hB}(\omega) \qquad (1)$$

with ϕ_{hB} and G^*_{hB} being the volume fraction and dynamic moduli for the matrix hB *in the blends*. For the blends containing rather small amount of the SB copolymers, the matrix behavior in the blends is hardly affected by the SB micelles. Thus, we replaced G^*_{hB} in eq 1 by the moduli for *pure* matrix (cf. dashed curves in Figure 1) and evaluated the SB contribution, $G^*_{SB}(\omega)$. For all blends examined, G^*_{SB} exhibited fast and slow relaxation processes. Both processes are attributed to relaxation of the SB micelles.

In previous studies,[2,3] the slow process was attributed to diffusion of the micelles but the molecular mechanism of the fast process was not specified. As in part 1,[1] we may relate the fast process to relaxation of individual B blocks tethered on the S cores. However, differing from blends examined in part 1, entanglements between the matrices and the corona B blocks should have effects on the fast process of the blends examined here. The remaining part of this paper mainly examines these effects on the basis of knowledge accumulated for entangled homopolymer blends.[4−17]

III.2. Mode Distribution for Fast Process. In part 1, the relative distribution of viscoelastic modes was found to be nearly universal for the fast process of the SB micelles in the nonentangling chB-2 matrix.[1] For the micelles in the entangling hB matrices, we examined whether a similar universality is observed for the reduced moduli, $G_r^* = [M_{bB}/c_{bB}RT]G^*_{SB}$ (cf. eq 1). Typical results are shown in Figures 2 and 3.

In Figure 2, the G_r^* curves of the concentrated SB 32−262/hB-28 blends ($c_{bB} > c_e$) are shifted along the ω axis by factors τ^* so that they are best superposed at around $\omega\tau^* = 1$. Good superposition is seen for G_r' at $\omega\tau^* \geq 1$, while G_r'' exhibits poorer superposition because of contribution of very rapid relaxation (at $\omega\tau^* \geq 100$). Subtraction of this contribution improved the superposition for G_r''. Although not shown here, G_r^* curves for concentrated blends of the other SB copolymers (Table 1) are also superimposed on the curves shown in Figure 2, and the quality of superposition was similar to that found in Figure 4 of part 1.[1] In the entangling hB matrices, magnitudes of G_r^* of those copolymers coincided with each other and no adjustment of the magnitudes was required for the superposition of the G_r^* curves. This result is different from those found in part 1 for the SB micelles in the short, nonentangling chB-2 matrix. At this moment, no clear explanation is found for this difference.

In Figure 3, the G_r' curves are shifted along the ω axis for *dilute* blends ($c_{bB} < c_e$) in various hB matrices. As done in Figure 2, the shift factors τ^* were chosen so that the curves were best superposed at around $\omega\tau^* = 1$. We note that the superposition is well achieved for $\omega\tau^* \geq 1$ (for the fast process) but scatter becomes prominent for $\omega\tau^* < 1$. This scatter is due to the low-ω tails of the G_r' curves observed most clearly for the SB 32−102 and 32−160 blends (squares and triangles). These low-ω tails correspond to the slow relaxation

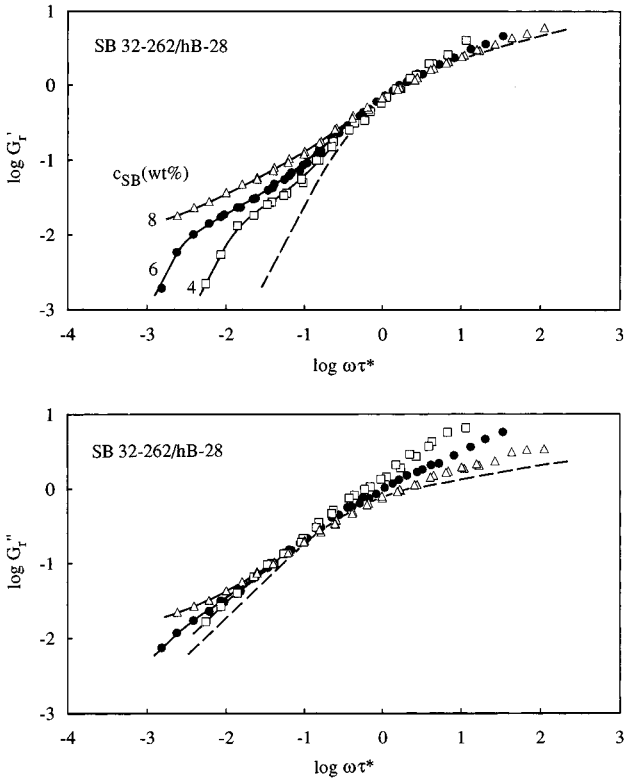

Figure 2. Plots of reduced moduli $G_r^* = [M_{bB}/c_{bB}RT]G^*_{SB}$ against reduced frequencies $\omega\tau^*$ for concentrated SB 32−262 micelles in the hB-28 matrix. Those micelles are entangled with each other through their B blocks as well as with the matrix hB-28. The dashed curves indicate reduced moduli for entangled 4-arm star hB (M_a = 48K),[18] $G_r^* = [M_a/cRT]G^*_{star}$, being plotted against $\omega\tau$ (τ = star relaxation time).

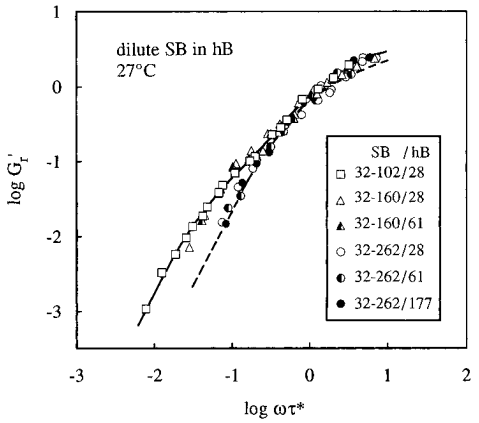

Figure 3. Plots of reduced moduli $G_r^* = [M_{bB}/c_{bB}RT]G^*_{SB}$ against reduced frequencies $\omega\tau^*$ for dilute SB micelles in various matrices as indicated. The micelles are entangled only with the matrix hB. The dashed curve is the same as that shown in Figure 2.

process of the dilute micelles (that is less prominent for SB 32−262 having larger M_{bB}).

The above results demonstrates nearly universal mode distribution (nearly identical shape of the G_r^* curves) for the fast relaxation process of the micelles in the entangling hB matrices. This distribution is further compared with the terminal mode distribution for a 4-arm star hB (of arm molecular weight M_a = 48K) reported by Raju et al.[18] In a wide range of concentration including both nonentangled and entangled regimes, this star hB exhibits (almost) identical shape of the G^* curve at low ω (cf. Figure 12 of ref 18). Thus, the G^* curve of the star hB in the entangled bulk state can be commonly compared with the curves for the dilute and concentrated micelles. For the star hB, plots of the reduced moduli $G_r^* = [M_a/cRT]G^*$ against $\omega\tau$ are shown with the dashed curves in Figures 2 and 3, where τ (= $J\eta$) is the terminal relaxation time of the star hB at 27 °C. The G_r^* curves were similar in magnitude for the star hB and the SB micelles in the entangling hB matrices, and no adjustment of the magnitude was carried out for the G_r^* curve of the star hB. (In part 1, the adjustment was required because of puzzling differences in the G_r^* magnitudes for the star hB and the SB micelles in the short chB-2 matrix.)

As seen in Figures 2 and 3, the G_r^* curves of the concentrated as well as dilute micelles are close to the dashed curves at $\omega\tau^* \geq 1$. Thus, the mode distribution for the fast process of these micelles is similar to that for the star hB, suggesting that this process is attributed to starlike relaxation of the B blocks irrespective of the micelle concentration.

III.3. Relaxation Time for Fast Process. In Figures 2 and 3, the relaxation time τ was used as the frequency shift factor for the G_r^* curve of the star hB. The superposition on this curve achieved for the SB micelles means that the shift factor τ^* gives the relaxation time for the fast process of the micelles. In fact, characteristic frequencies τ^{*-1} (cf. diamonds in Figure 1) specify well the low-ω end of the fast process. As explained in part 1, τ^* may contain uncertainties as large as $\Delta \log \tau^* = 0.3$. However, those τ^* data are still sufficient for the argument in this paper.

Extensive experiments for homopolymer blends[5−17] indicate that *dilute* probe chains being entangled only with *much shorter* matrix chains relax via a constraint release (CR) mechanism.[19−21] For blends of dilute star hB chains in linear hB matrices, Roovers[17] reported data for the CR relaxation time τ_{CR} (at 27 °C). Regarding the B blocks of the SB micelles as an arm for star hB, we interpolated his data (Figure 7 of ref 17) to estimate τ_{CR} for the B blocks. (Roovers[17] defined his relaxation time as a reciprocal frequency at which dynamic compliance decreased to 90% of its low-ω asymptotic value, while our relaxation time is defined as the product $J\eta$ often referred to as a *weight-average* relaxation time. We evaluated ratios of the two differently defined relaxation times for the data of Roovers[17] and used the ratios to estimate τ_{CR} according to our definition.)

In Figure 4, the estimated τ_{CR} is compared with τ^* for *dilute* micelles having B blocks entangled only with the matrix hB (cf. Figure 3). Clearly, τ^* is proportional to τ_{CR}. In addition, τ^* is close to τ_{CR} in magnitude. These results strongly suggest that the fast process for the dilute micelles is attributed to the CR relaxation of individual B blocks that is induced by the matrix motion.

For concentrated blends in which neighboring micelles are entangled through their B blocks, Figure 5 shows semilogarithmic plots of τ^*_{conc} for the fast process against the B block concentration c_{bB} in the matrix phase. The unfilled and filled symbols indicate τ^*_{conc} for the micelles in the entangling hB and nonentangling chB-2 matrices, respectively. (The τ^*_{conc} data in the chB-2 matrix[1] are compared at an isofrictional state). The horizontal dashed lines indicate τ^*_{dil} for the dilute micelles examined in Figure 4.

In Figure 5, we first note that τ^*_{conc} is almost the same in the hB-28 and chB-2 matrices, the former being entangled with the B blocks while the latter forms no entanglements (cf. circles and squares). Thus, entangle-

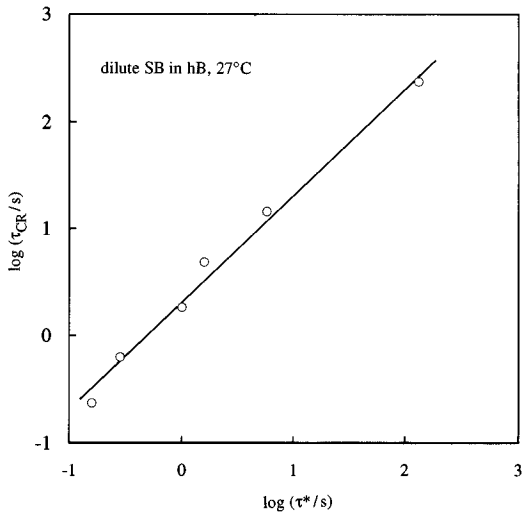

Figure 4. Comparison of the relaxation time τ^* for the fast process of dilute micelles with the constraint release relaxation time τ_{CR} for B blocks. τ_{CR} was estimated from the data of Roovers[17] for dilute star hB chains in linear hB matrices.

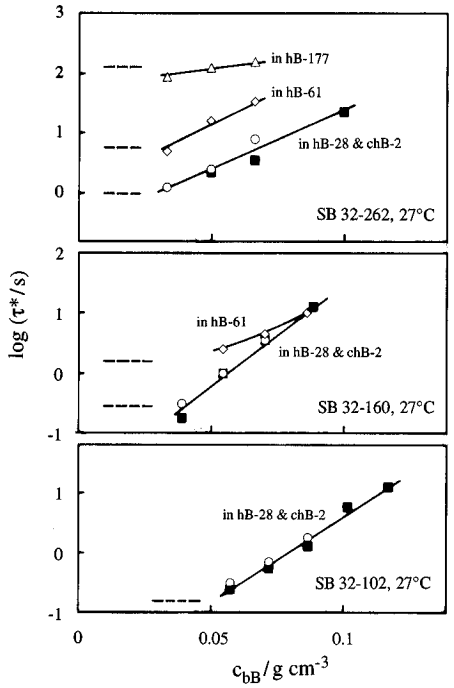

Figure 5. Dependence of the relaxation time τ^* for the fast process of concentrated SB micelles on the B block concentration c_{bB} in the entangling hB matrices (unfilled symbols). Those micelles are entangled with each other through their B blocks. The filled squares indicate the τ^* data for the concentrated micelles in the nonentangling chB-2 matrix[1] reduced at the isofrictional state. The horizontal lines represent the τ^* data for dilute micelles (cf. Figure 4).

ments due to hB-28 appears to have no effect for τ^*_{conc}. However, in longer hB-61 and hB-177 matrices, τ^*_{conc} becomes longer and its c_{bB} dependence becomes weaker. In particular, in the hB-177 matrix (cf. triangles), τ^*_{conc} is almost independent of c_{bB} and close to τ^*_{dil} and thus to τ_{CR} in the entire range of c_{bB} examined. Knowledge accumulated for homopolymer blends[5−12] enables us to understand these results in the following way.

In the concentrated blends, each B block has two types of entanglements, one with the matrix hB and the other with B blocks of neighboring micelles. Thus, relaxation of the B block is achieved only when both types of entanglements become ineffective. For this relaxation, the following three modes are potentially available, (1) retarded Rouse-like CR relaxation due to the matrix motion, (2) starlike arm retraction of the B block trapped in a sparse entanglement mesh formed only by B blocks of neighboring micelles, and (3) the arm retraction in a denser, bulk entanglement mesh formed by both matrix and B blocks of neighboring micelles. Obviously, the arm retraction in the sparse mesh can take place only after the entanglement due to the matrix becomes ineffective *via* the CR mode (1). Thus, the arm retraction mode (2) determines the relaxation rate of the B blocks only when this mode is much slower than the CR mode. This criterion is satisfied only for B blocks being entangled with *sufficiently shorter* matrix. For this case, the matrix behaves just as a diluent at time scales of τ^*_{conc} and the terminal relaxation of the B blocks is governed by the arm retraction in the sparse mesh. This leads to M_{hB}-independent τ^*_{conc} that increases exponentially with c_{bB} (like τ for entangled star chains[1]), being in harmony with the result found for the SB micelles in hB-28 and chB-2 (cf. circles and squares in Figure 5).

On the other hand, if the matrix becomes sufficiently long, the CR mode becomes much slower than the arm retraction mode in the sparse mesh. For this case, the relaxation rate of the B blocks is determined by competition of the CR mode (1) and the arm retraction mode (3) in the dense mesh. Differing from star hB chains, the B blocks are tethered on the impenetrable S cores that constrain the B block relaxation.[1] Thus, the mode (3) is tremendously slow for the B blocks, and the CR mode becomes dominant for the B block relaxation. For complete relaxation of the B blocks, the CR relaxation of the entanglement due to the long matrices should take place first and then the entanglement between the B blocks should relax *via* the arm retraction *in the sparse mesh*. However, this arm retraction time is negligible as compared to the CR time in the long matrices. Thus, the CR mode determines the B block relaxation rate, thereby leading to the c_{bB}-insensitive τ^*_{conc} that is close to τ_{CR} (cf. triangles and dashed line in Figure 5).

As explained above, the fast process of the SB micelles in the entangling hB matrices is quite possibly due to starlike relaxation of the B blocks, and the CR effects on this relaxation change with c_{bB}, M_{bB}, and M_{hB}. Concerning this point, we also have to emphasize a quantitative difference between the B blocks and stars: The relaxation is significantly slower for the B blocks tethered on the S cores than for corresponding hB stars.[1] This difference can be related to effects of the impenetrable S cores that constrain the *retraction* of the B blocks.[1] This in turn means that the CR relaxation is more easily realized for the B blocks than for star hB, because the Rouse-like CR motion of the B blocks would hardly be affected by the S cores and thus easily overwhelm the constrained and retarded retraction of the B blocks.

III.4. Relaxation Time for Slow Processes. We here examine the mechanim(s) for the slow relaxation process of the SB micelles in the entangling hB matrices. For the simplest case in which this process is governed by the Stokes−Einstein (SE) diffusion of the micelles, the relaxation times of the slow process, τ_s, should be close to the SE diffusion time discussed in part 1,

$$\tau_{SE} = \pi R_m \eta_{eff} \delta^2 / kT \qquad (2)$$

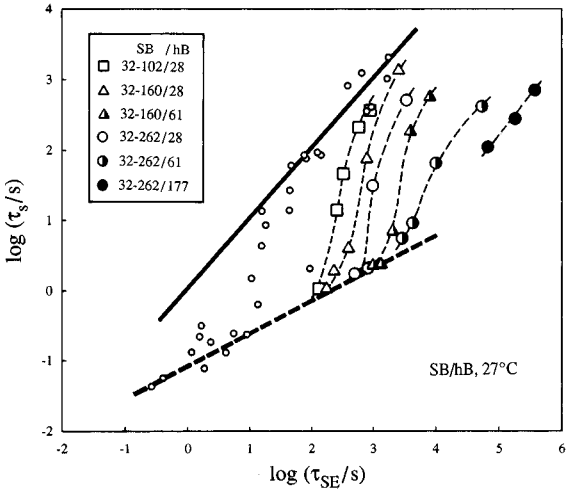

Figure 6. Plots of the relaxation time τ_s for the slow process of the SB micelles in the entangling hB matrices against the Stokes−Einstein diffusion time τ_{SE} evaluated for $\eta_{eff} = \eta_{fast}$ (large symbols). The small circles indicate the plots for the micelles in the nonentangling chB-2 matrix at the isofrictional state.[1] The thick solid line indicates the relationship $\tau_s = \tau_{SE}$.

Here, R_m and δ are the micelle radius and diffusion distance, respectively, and η_{eff} is an effective viscosity for the micelle diffusion. The R_m and δ values evaluated in part 1 were used also for the micelles in the entangling matrices examined here.

As in part 1, we replaced η_{eff} in eq 2 by the viscosities η_{fast} for the fast process of the micelles that reflects relaxation of individual B blocks. In the entangling hB matrices examined here, the fast process is observed in our experimental window for both dilute and concentrated micelles and the G_r* curves for this process are well superposed on the curve for the star hB of M_a = 48K (cf. Figures 1−3). Thus, we evaluated η_{fast} for both cases from the known viscosity of the star hB.

As in part 1, τ_s for the micelles in the entangling hB matrices were evaluated from the low-ω tails of G'_{SB} and G''_{SB},

$$\tau_s = J_{SB}\eta_{SB}, \quad \eta_{SB} = [G''_{SB}/\omega]_{\omega\to 0}, \quad J_{SB} = \eta_{SB}^{-2}[G'_{SB}/\omega^2]_{\omega\to 0} \quad (3)$$

Characteristic frequencies, τ_s^{-1}, are well located at the low-ω end of the slow process (cf. arrows in Figure 1). In Figure 6, those τ_s data are compared with τ_{SE} being evaluated for $\eta_{eff} = \eta_{fast}$ (large symbols). The small symbols indicate the data for the micelles in the nonentangling chB-2 matrix.[1] The thick solid line represents the relationship $\tau_s = \tau_{SE}$.

As found in part 1, τ_s for the SB micelles in the nonentangling chB-2 matrix increase with increasing c_{SB} from the low-c_{SB} asymptotic values (thick dashed line in Figure 6) to the high-c_{SB} asymptotic values being close to τ_{SE} (thick solid line). Figure 6 suggests a similar behavior for respective series of the SB micelles in the entangling hB matrices. Thus, in both nonentangling and entangling matrices, the SE mechanism appears to dominate the slow relaxation process of the concentrated micelles being entangled through their B blocks. However, Figure 6 also indicates that the asymptotic SE behavior is more difficult to be attained in longer matrices. (For example, compare τ_s for the SB 32−262 micelles in the three different hB matrices.) At this moment, no explanation is found for this matrix effect.

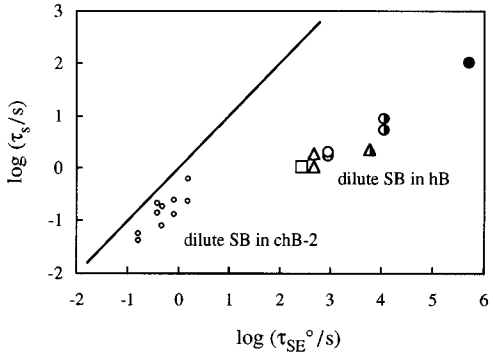

Figure 7. Plots of the relaxation time τ_s for the slow process of the *dilute* SB micelles in the entangling and nonentangling hB matrices against the Stokes−Einstein diffusion time τ_{SE}° evaluated for $\eta_{eff} = \eta_{mat}$. The symbols are the same as in Figure 6. The solid line indicates the relationship $\tau_s = \tau_{SE}$°.

In Figure 6, we also note that τ_s for the dilute micelles are significantly shorter than τ_{SE} evaluated for $\eta_{eff} = \eta_{fast}$. The use of η_{fast} in the evaluation of τ_{SE} corresponds to a hypothesis that the diffusion of the micelles takes place only after the relaxation of individual B blocks is completed. This hypothesis can be justified for the concentrated micelles entangled through their B blocks, because the SE diffusion should be disturbed when the B blocks have not yet relaxed and elastic forces are acting between neighboring micelles through those B blocks. However, the hypothesis is not necessarily valid for dilute and nonoverlapping micelles that are not subjected to those elastic forces. Thus, one might expect that η_{eff} for the dilute micelles are given by the matrix viscosity η_{mat}, not by η_{fast} for relaxation of individual B blocks, and that τ_s is close to τ_{SE}° evaluated for $\eta_{eff} = \eta_{mat}$,

$$\tau_{SE}^{\circ} = \pi R_m \eta_{mat}\, \delta^2/kT \quad (4)$$

This expectation is examined in Figure 7 where τ_s for the dilute micelles are plotted against τ_{SE}°. The solid line represents the relationship $\tau_s = \tau_{SE}$°. The symbols are the same as in Figure 6.

As seen in Figure 7, τ_s is fairly close to τ_{SE}° for the micelles in the nonentangling chB-2 matrix (cf. small circles and solid line). This result appears to support the above expectation. However, τ_s is orders of magnitude shorter than τ_{SE}° for the micelles in the entangling matrices (large symbols), meaning that some relaxation mode much faster than the SE diffusion is available for those micelles. It should be also noted that τ_s is not proportional to τ_{SE}° and thus not to η_{mat} for a particular SB micelle. (For example, compare the unfilled, half filled, and fully filled large circles for the SB 32−262 micelle in the three hB matrices.) Thus, the slow relaxation processes of the dilute micelles *might* be attributed to their SE diffusion for the limited case of the nonentangling matrix but not for general cases including both entangled and nonentangled matrices. The data seen in Figure 7 are not sufficient to judge whether the slow relaxation mechanism for the dilute micelles is common (and not of the SE nature) in both matrices or the mechanism changes with the matrix entanglements. Further studies are necessary for this problem.

IV. Concluding Remarks

For the SB micelles in long hB matrices, we have examined effects of entanglements between the matrix

and B blocks on the fast relaxation process of the micelles. For dilute micelles, this process is attributed to the CR relaxation of the corona B blocks due to the matrix motion (cf. Figure 4). For concentrated micelles being entangled through the B blocks, the fast process is still attributed to relaxation of individual B blocks but the relaxation mechanism appears to change with the matrix M_{hB}: In sufficiently short matrices, the entanglements due to the matrices rapidly relax *via* the CR mechanism and the B block appears to relax *via* the starlike retraction in a sparse entanglement mesh formed by neighboring B blocks. On the other hand, in sufficiently long matrices, the CR relaxation becomes dominant even for the B blocks of concentrated micelles. These molecular pictures explain features of the fast relaxation process (Figure 5). However, quantitative differences exist for the relaxation times of the B blocks and star hB.[1] These differences, possibly reflecting the effects of the S cores, deserve further attention.

For concentrated SB micelles in the relatively short matrices, entanglements with the matrices barely affect the slow relaxation mechanism: For those micelles, the Stokes−Einstein diffusion appears to govern the slow process. However, with increasing matrix length, the SE behavior becomes more difficult to be attained. In addition, for dilute micelles in nonentangling and entangling matrices, the SE mechanism does not consistently explain features of the slow process (Figure 7). Further studies are desired for the mechanism(s) of the slow process.

References and Notes

(1) Watanabe, H.; Sato, T.; Osaki, K. *Macromolecules* **1996**, *29*, 104.
(2) Watanabe, H.; Kotaka, T. *Macromolecules* **1983**, *16*, 769.
(3) Watanabe, H.; Kotaka, T. *Macromolecules* **1984**, *17*, 342.
(4) For earlier work on binary polymer blends, see: Ferry, J. D. *Viscoelastic Properties of Polymers*, 3rd ed.; Wiley: New York, 1980; Chapter 13.
(5) Watanabe, H.; Kotaka, T. *Macromolecules* **1984**, *17*, 2316.
(6) Watanabe, H.; Sakamoto, T.; Kotaka, T. *Macromolecules* **1985**, *18*, 1008, 1436.
(7) Watanabe, H.; Kotaka, T. *Macromolecules* **1986**, *19*, 2520.
(8) Watanabe, H.; Yoshida, H.; Kotaka, T. *Macromolecules* **1988**, *21*, 2175.
(9) Yoshida, H.; Watanabe, H.; Kotaka, T. Macromolecules **1991**, *24*, 572.
(10) Watanabe, H.; Yamazaki, M.; Yoshida, H.; Kotaka, T. *Macromolecules* **1991**, *24*, 5573.
(11) Watanabe, H.; Kotaka, T. *CHEMTRACTS Macromol. Chem.* **1991**, *2*, 139.
(12) Watanabe, H.; Yoshida, H.; Kotaka, T. *Macromolecules* **1992**, *25*, 2442.
(13) Montfort, J.-P.; Marin, G.; Monge, P. *Macromolecules* **1984**, *17*, 1551.
(14) Montfort, J.-P.; Marin, G.; Monge, P. *Macromolecules* **1986**, *19*, 1979.
(15) Strunglinski, M. J.; Graessley, W. W. *Macromolecules* **1985**, *18*, 2630.
(16) Struglinski, M. J.; Graessley, W. W.; Fetters, L. J. *Macromolecules* **1988**, *21*, 783.
(17) Roovers, J. *Macromolecules* **1987**, *20*, 148.
(18) Raju, V. R.; Menezes, E. V.; Marin, G.; Graessley, W. W.; Fetters, L. J. *Macromolecules* **1981**, *14*, 1668.
(19) Klein, J. *Macromolecules* **1978**, *11*, 852.
(20) Graessley, W. W. *Adv. Polym. Sci.* **1982**, *47*, 67.
(21) Watanabe, H.; Tirrell, M. *Macromolecules* **1989**, *22*, 927.

MA951250G